Journal of Geodesy (1998) 72: 684–697

Journal of Geodesy

Performance of three types of Stokes's kernel in the combined solution for the geoid

P. Vaníček[1], W. E. Featherstone[2]

[1] Department of Geodesy and Geomatics Engineering, University of New Brunswick, P.O. Box 4400, Fredericton, New Brunswick, E3B 5A3, Canada e-mail: vanicek@unb.ca; Tel: +1 506 453 4698; Fax: +1 506 453 4943
[2] School of Spatial Sciences, Curtin University of Technology, GPO Box U1987, Perth, WA 6845, Australia
e-mail: Featherstone_WE@cc.curtin.edu.au; Tel: +61 8 9266 2734; Fax: +61 8 9266 2703

Received: 11 August 1997 / Accepted: 18 August 1998

Abstract. When regional gravity data are used to compute a gravimetric geoid in conjunction with a geopotential model, it is sometimes implied that the terrestrial gravity data correct any erroneous wavelengths present in the geopotential model. This assertion is investigated. The propagation of errors from the low-frequency terrestrial gravity field into the geoid is derived for the spherical Stokes integral, the spheroidal Stokes integral and the Molodensky-modified spheroidal Stokes integral. It is shown that error-free terrestrial gravity data, if used in a spherical cap of limited extent, cannot completely correct the geopotential model. Using a standard norm, it is shown that the spheroidal and Molodensky-modified integration kernels offer a preferable approach. This is because they can filter out a large amount of the low-frequency errors expected to exist in terrestrial gravity anomalies and thus rely more on the low-frequency geopotential model, which currently offers the best source of this information.

Key words. Geoid determination · Modified kernels · Error propagation · High-pass filtering

1 Introduction

Formally, Stokes's integral must be evaluated over the whole Earth using gravity anomalies that have been downward-continued to the geoid, which is assumed to be spherical, to give the gravimetric geoid height (N) at a single point. This is

$$N = \kappa \int_0^{2\pi} \int_0^{\pi} S(\psi) \Delta g \sin\psi \, \mathrm{d}\psi \, \mathrm{d}\alpha \tag{1}$$

where $\kappa = R/(4\pi\gamma)$, R is the mean Earth radius, γ is normal gravity on the reference ellipsoid, (ψ, α) are the spherical distance and azimuth, respectively, of each gravity anomaly (Δg)[1] from each computation point, and $S(\psi)$ is the spherical Stokes kernel, which is given by an infinite Fourier series of Legendre polynomials, $P_n(\cos\psi)$, as

$$S(\psi) = \sum_{n=2}^{\infty} \frac{2n+1}{n-1} P_n(\cos\psi) \tag{2}$$

The orthogonality relations between Legendre polynomials over the sphere allow Eq. (1) to be expressed in its spectral form as

$$N = c \sum_{n=2}^{\infty} \frac{2}{n-1} \Delta g_n \tag{3}$$

where $c = R/(2\gamma)$ and Δg_n is the n-th degree surface spherical harmonic of the gravity anomalies. In practice, these are computed using a set of fully normalised potential coefficients that define a global geopotential model, such that

$$\Delta g_n^G = \frac{GM}{r^2} \left(\frac{a}{r}\right)^n (n-1) \sum_{m=0}^{n} (\delta \overline{C}_{nm} \cos m\lambda + \overline{S}_{nm} \sin m\lambda) \times \overline{P}_{nm}(\cos\theta) \tag{4}$$

where GM is the product of the Newtonian gravitational constant and mass of the Earth, a is the equatorial radius of the reference ellipsoid, (r, θ, λ) are the geocentric polar coordinates of each computation point, $\delta\overline{C}_{nm}$ and $\overline{S}_{nm}$ are the fully normalised potential coefficients of degree n and order m, which have been reduced by the even zonal harmonics of the reference ellipsoid, and $\overline{P}_{nm}(\cos\theta)$ are the fully normalised associated Legendre functions.

Using Eq. (4) in Eq. (3) for the region $2 \le n \le M$ gives the low-frequency contribution of the potential coefficients to the geoid as

[1] The derivation or exact kind of gravity anomalies are not discussed in this paper.

$$N_M = c\sum_{n=2}^{M}\frac{2}{n-1}\Delta g_n^G = \frac{GM}{r\gamma}\sum_{n=2}^{M}\left(\frac{a}{r}\right)^n\sum_{m=0}^{n}(\delta\overline{C}_{nm}\cos m\lambda + \overline{S}_{nm}\sin m\lambda)\overline{P}_{nm}(\cos\theta) \quad (5)$$

where M is the degree of some spherical harmonic expansion of the geopotential model.

The incomplete global coverage of terrestrial gravity data has driven the use of a geopotential model in the determination of the geoid. This has been called the generalised Stokes scheme by Vaníček and Sjöberg (1991). Such an approach reduces the effect of not using a global coverage of terrestrial gravity data and also reduces the impact of the spherical approximations inherent to Stokes's formula (Heiskanen and Moritz 1967, p. 97). The latter is achieved because most of the geoid's power is contained within the low frequencies; see Eq. (3).

However, the combination of a geopotential model with terrestrial gravity data in a spherical cap of limited extent via Stokes's integral is sometimes presented in a way that implies that the terrestrial gravity data improve any errors present in the geopotential model (e.g. Sideris and Schwarz 1987). This assertion is examined in this paper by comparing three implementations of Stokes's integration when combined with a geopotential model. These comprise the use of the spherical Stokes kernel (Eq. 2), the spheroidal Stokes kernel and the Molodensky modified Stokes kernel (Vaníček and Kleusberg 1987). Other modifications to Stokes kernel exist, such as those of Meissl (1971), Sjöberg (1984, 1986, 1991), Heck and Grüninger (1987), Vaníček and Sjöberg (1991), and Featherstone et al. (1998), but they will not be discussed here for lack of space. However, they will be discussed in a sequel to this paper, which is currently in preparation.

By transforming these Stokes's integrals to the frequency domain, in terms of surface spherical harmonics, it will be shown that when the terrestrial gravity anomalies are used from a region of limited extent, they can only correct the low-frequency errors present in the geopotential model to a limited extent. It will also be shown that the impact on the geoid of the low-frequency errors, known to be present in the terrestrial gravity anomalies, can be reduced when the spheroidal or Molodensky-modified forms of Stokes's integral are used.

2 The spherical Stokes kernel

Many authors combine a global geopotential model – typically to maximum degree and order $M = 360$ – with regional gravity data using the spherical Stokes kernel, Eq. (2). In this instance, the geoid is estimated via

$$N_1 = N_M + \kappa\int_0^{2\pi}\int_0^{\psi_o} S(\psi)\Delta g^M \sin\psi\ \mathrm{d}\psi\ \mathrm{d}\alpha \quad (6)$$

where the Stokes integration is performed over a limited surface spherical cap bound by ψ_o. This also uses only the high-frequency gravity anomalies (Δg^M), which are terrestrial gravity anomalies (Δg^T) that have been reduced by the gravity anomalies implied by a geopotential model (Δg^G) of spherical harmonic degree and order (M) according to

$$\Delta g^M = \Delta g^T - \sum_{n=2}^{M}\Delta g_n^G \quad (7)$$

One objective of this paper is to express Eq. (6) completely in a spectral form, using spherical harmonics, so that the propagation of errors into the geoid from the two sources of gravity field information may be investigated. In order to achieve this in a straightforward manner, the spherical Stokes kernel, Eq. (2) as used in Eq. (6) is expressed as

$$\overline{S}(\psi,\psi_o) = \begin{cases} S(\psi) & \text{for } 0 \le \psi \le \psi_o \\ 0 & \text{for } \psi_o < \psi \le \pi \end{cases} \quad (8)$$

As with Eq. (2), Eq. (8) can be expressed as an infinite Fourier series of Legendre polynomials by

$$\overline{S}(\psi,\psi_o) = \sum_{n=2}^{\infty}\frac{2n+1}{2}s_n(\psi_o)P_n(\cos\psi) \quad (9)$$

where $s_n(\psi_o)$ are coefficients which will be derived later in this section.

Using Eq. (8) in Eq. (6) yields an identical relationship to Eq. (6), except that the integration domain is now over the whole Earth (sphere), viz.

$$N_1 = N_M + \kappa\int_0^{2\pi}\int_0^{\pi}\overline{S}(\psi,\psi_o)\Delta g^M\sin\psi\ \mathrm{d}\psi\ \mathrm{d}\alpha \quad (10)$$

Equations (5) and (9) are substituted in Eq. (10), and then using the orthogonality relations to replace the integral term yields

$$N_1 = c\sum_{n=2}^{M}\frac{2}{n-1}\Delta g_n^G + c\sum_{n=2}^{M}s_n(\psi_o)\Delta g_n^M + c\sum_{n=M+1}^{\infty}s_n(\psi_o)\Delta g_n^M \quad (11)$$

The preceding mathematical development has disregarded the fact that all the gravity anomaly harmonics used are only estimates of their true values, due to the existence of measurement and data reduction errors, for instance. Therefore, the gravity anomalies used in Eq. (11) must be replaced by their estimates from the geopotential model ($\Delta\hat{g}_n^G$) and the terrestrial gravity observations ($\Delta\hat{g}_n^T$). As the terrestrial gravity data have already been reduced by the geopotential model [according to Eq. (7)], this gives the estimate of the geoid as

$$\hat{N}_1 = c\sum_{n=2}^{M}\frac{2}{n-1}\Delta\hat{g}_n^G + c\sum_{n=2}^{M}s_n(\psi_o)(\Delta\hat{g}_n^T - \Delta\hat{g}_n^G) + c\sum_{n=M+1}^{\infty}s_n(\psi_o)\Delta\hat{g}_n^T \quad (12)$$

From Eq. (12), it is evident that the propagation of errors into the geoid from the geopotential model and terrestrial gravity data is controlled, in part, by the coefficients $s_n(\psi_o)$. Therefore, it is important to have a knowledge of their magnitudes. This can be achieved through a rearrangement of Eq. (9) using the orthogonality relations over the sphere, such that

$$s_n(\psi_o) = \int_0^{\pi} \overline{S}(\psi, \psi_o) P_n(\cos\psi) \sin\psi \, \mathrm{d}\psi \tag{13}$$

Introducing the spherical (Molodensky et al. 1962) truncation coefficients

$$Q_n(\psi_o) = \int_{\psi_o}^{\pi} S(\psi) P_n(\cos\psi) \sin\psi \, \mathrm{d}\psi \tag{14}$$

and using these, together with the relation of Eq. (8), in Eq. (13) yields

$$\begin{aligned} s_n(\psi_o) &= \int_0^{\pi} S(\psi) P_n(\cos\psi) \sin\psi \, \mathrm{d}\psi - Q_n(\psi_o) \\ &= \frac{2}{n-1} - Q_n(\psi_o) \quad \forall n \geq 2 \end{aligned} \tag{15}$$

Substituting this result in Eq. (12) produces

$$\begin{aligned} \hat{N}_1 = c \sum_{n=2}^{M} \left[Q_n(\psi_o) \Delta\hat{g}_n^G + \left(\frac{2}{n-1} - Q_n(\psi_o) \right) \Delta\hat{g}_n^T \right] \\ + c \sum_{n=M+1}^{\infty} \left(\frac{2}{n-1} - Q_n(\psi_o) \right) \Delta\hat{g}_n^T \end{aligned} \tag{16}$$

Next, the degree-errors in the geopotential model-derived gravity anomalies (ϵ_n^G) and the terrestrial gravity anomalies (ϵ_n^T) are introduced into Eq. (16) to yield

$$\begin{aligned} \hat{N}_1 = c \sum_{n=2}^{M} \Big[& Q_n(\psi_o) \{ \Delta g_n^G + \epsilon_n^G \} \\ & + \left(\frac{2}{n-1} - Q_n(\psi_o) \right) \{ \Delta g_n^T + \epsilon_n^T \} \Big] \\ & + c \sum_{n=M+1}^{\infty} \left(\frac{2}{n-1} - Q_n(\psi_o) \right) \{ \Delta g_n^T + \epsilon_n^T \} \end{aligned} \tag{17}$$

where the superscripts G and T are retained simply to indicate the source of the gravity anomalies. Subtracting Eq. (3) from Eq. (17) $\forall n \geq 2$ leaves the error that occurs in the geoid (ϵ_{N1}) when terrestrial gravity anomalies and geopotential coefficients are combined to compute the geoid using the approach given in Eq. (6). This is

$$\begin{aligned} \epsilon_{N1} = c \sum_{n=2}^{M} \left[\frac{2}{n-1} \epsilon_n^T + Q_n(\psi_o) \left(\epsilon_n^G - \epsilon_n^T \right) \right] \\ + c \sum_{n=M+1}^{\infty} \left[\frac{2}{n-1} \epsilon_n^T - Q_n(\psi_o) \Delta g_n^T - Q_n(\psi_o) \epsilon_n^T \right] \end{aligned} \tag{18}$$

For convenience during the subsequent comparisons, Eq. (18) is rewritten so as to distinguish the error contribution to the geoid from the errors in the terrestrial gravity data, errors in the geopotential coefficients, and the truncation error associated with the limited integration domain (ψ_o) in Eq. (6), respectively. This gives

$$\begin{aligned} \epsilon_{N1} = c \sum_{n=2}^{\infty} \left(\frac{2}{n-1} - Q_n(\psi_o) \right) \epsilon_n^T + c \sum_{n=2}^{M} Q_n(\psi_o) \epsilon_n^G \\ - c \sum_{n=M+1}^{\infty} Q_n(\psi_o) \Delta g_n^T \end{aligned} \tag{19}$$

The truncation error, or remote zone contribution, comprises the last term in Eq. (19), and represents a bias that must be considered when using Eq. (6) to compute the geoid. It results from the neglect of high-frequency ($n > M$) gravity anomalies in the remote zones outside the integration domain ($\psi_o < \psi \leq \pi$). As this discussion is only concerned with the question of how the terrestrial gravity data can attenuate any errors in the geopotential model, the truncation error term need not be considered as it only affects the high-frequency gravity field.

Figure 1a shows the magnitudes of the coefficients that control the propagation of the degree-errors from the geopotential model (ϵ_n^G) and the terrestrial gravity anomalies (ϵ_n^T) through Eq. (19) in relation to the generic $2/(n-1)$ term [cf. Eq. (3)]. This generic term shows how the errors propagate if the original Stokes integral, Eq. (1), is used to compute the geoid. The spherical truncation coefficients, Eq. (14), were computed using the recursive routines of Paul (1973). The values of $M = 360$ and $\psi_o = 6^\circ$ were chosen as they provide a representative example to show the relative magnitude of the terms in Eq. (19).

In Fig. 1a, the dominance of the generic $2/(n-1)$ term, which is asymptotic, tends to obscure the behaviour of the coefficients in the high degrees. Therefore, a normalisation has been used to produce Fig. 1b, where each coefficient is multiplied by $(n-1)/2$; the inverse of the so-called generic term. In Fig. 1b, the generic term becomes unity, the spherical truncation coefficients that apply to error in the geopotential model (ϵ_n^G) oscillate about zero, and the coefficients that apply to the terrestrial gravity data errors (ϵ_n^T) oscillate about unity. This form of presentation allows a clearer comparison among the three approaches investigated (see later).

2.1 Special cases of Eq. (19)

Next, three special cases of Eq. (19) are considered. The first is for integration of Eq. (6) over the whole Earth (i.e. $\psi_o = \pi$), where the spherical truncation coefficients reduce to $Q_n(\pi) = 0, \ \forall n \geq 2$. This can be proven from Eq. (14) using the orthogonality relations between Legendre polynomials over the sphere. Thus, Eq. (19) reduces to

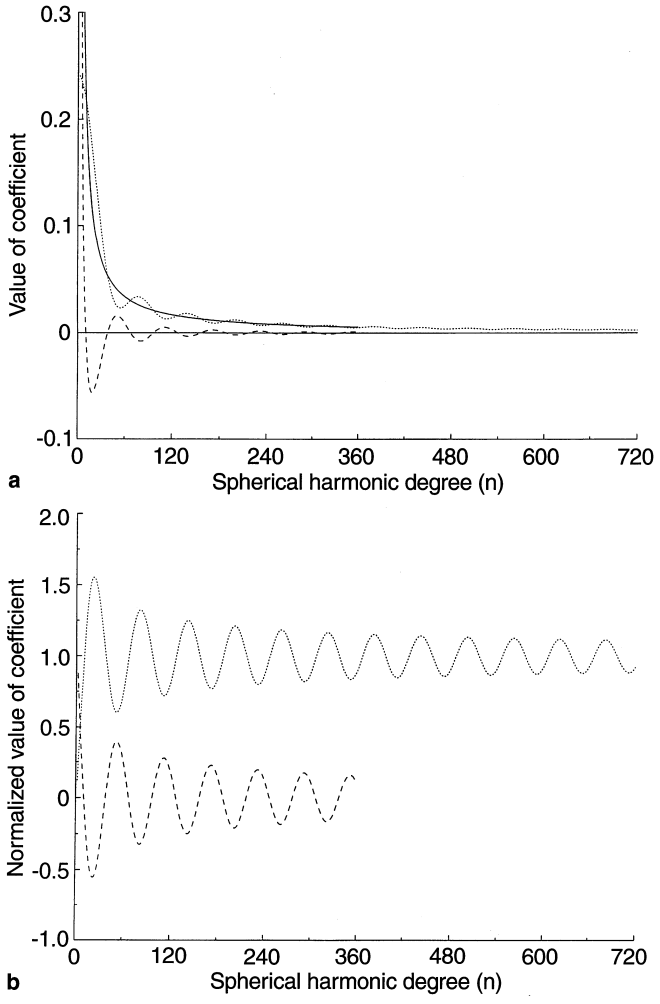

Fig. 1. a The generic $2/(n-1)$ term $\forall n \geq 2$ (*solid line*), the spherical truncation coefficients $Q_n(6^\circ)$ for $2 \leq n \leq 360$ (*dashed line*), and their difference $(2/(n-1) - Q_n(6^\circ))$ for $n \geq 2$ (*dotted line*). **b** The normalised spherical truncation coefficients $((n-1)/2)Q_n(6^\circ))$ for $2 \leq n \leq 360$ (*dashed line*), and their normalised difference $((n-1)/2)(2/(n-1) - Q_n(6^\circ))$ for $n \geq 2$ (*dotted line*)

$$\epsilon_{N1} = c \sum_{n=2}^{\infty} \frac{2}{n-1} \epsilon_n^T \tag{20}$$

Equation (20) shows that when terrestrial gravity data are used over the whole Earth in Eq. (6), the resulting error in the geoid is controlled entirely by the generic $2/(n-1)$ term, as if the original Stokes formula, Eq. (1), had been used over the whole Earth [cf. Eqs. (20) and (3)]. Note also that the truncation error reduces to zero in this instance, as would be expected. Curiously, this result is equivalent to completely disregarding the geopotential model during the geoid computations.

In the case of no Stokes integration [i.e. $\psi_o = 0$ in Eq. (6)], the spherical truncation coefficients attain their maximum value of $Q_n(0) = \frac{2}{n-1}$, $\forall n \geq 2$. Again, this can be proven from Eq. (14) in conjunction with the orthogonality relations between Legendre polynomials over the sphere. Thus, Eq. (19) becomes

$$\epsilon_{N1} = c \sum_{n=2}^{M} \frac{2}{n-1} \epsilon_n^G - c \sum_{n=M+1}^{\infty} \frac{2}{n-1} \Delta g_n^T \tag{21}$$

where the truncation error [second term on the right-hand side of Eq. (21)] attains its maximum value, and the error from the geopotential passes undiminished into the geoid according to the generic $2/(n-1)$ term. This result gives an error equivalent to using only the geopotential model to compute the geoid [cf. Eqs (21) and (5)]. Also, the truncation error term in Eq. (21) is equal to the omission error of the geopotential model.

When an error-free geopotential model is considered (i.e. $\epsilon_n^G = 0$ for $2 \leq n \leq M$), together with the Stokesian integration over a cap bound by ψ_o, Eq. (19) reduces to

$$\begin{aligned} \epsilon_{N1} = c \sum_{n=2}^{\infty} \left(\frac{2}{n-1} - Q_n(\psi_o) \right) \epsilon_n^T \\ - c \sum_{n=M+1}^{\infty} Q_n(\psi_o) \Delta g_n^T \end{aligned} \tag{22}$$

Equation (22) shows that the terrestrial gravity data errors propagate into the geoid $\forall n \geq 2$, and are controlled by the coefficients $(2/(n-1) - Q_n(\psi_o))$; see Fig. 1a, b. Therefore, even if the geopotential model is error-free, the inclusion of terrestrial gravity data via Eq. (6) allows low-frequency ($2 \leq n \leq M$) terrestrial gravity anomaly errors to leak into the solution and thus degrade the geoid in this region.

3 The spheroidal Stokes kernel

The spherical Stokes kernel, Eq. (2), used in Eq. (6) is now replaced by its spheroidal counterpart. This is referred to as the spheroidal Stokes kernel by Vaníček and Kleusberg (1987) and Vaníček and Sjöberg (1991). In this approach, the low-degree Legendre polynomials ($2 \leq n \leq M$) are removed from the spherical Stokes kernel to yield

$$\begin{aligned} S^M(\psi) &= S(\psi) - \sum_{n=2}^{M} \frac{2n+1}{n-1} P_n(\cos\psi) \\ &= \sum_{n=M+1}^{\infty} \frac{2n+1}{n-1} P_n(\cos\psi) \end{aligned} \tag{23}$$

Using this spheroidal kernel gives the estimate of the geoid as

$$N_2 = N_M + \kappa \int_0^{2\pi} \int_0^{\psi_o} S^M(\psi) \Delta g^M \sin\psi \, \mathrm{d}\psi \, \mathrm{d}\alpha \tag{24}$$

Note that in Eq. (24), the degree of the spheroidal kernel has been chosen to equal the degree by which the terrestrial gravity anomalies have been reduced [Eq. (7)]. In this discussion, the spheroidal kernel is used as the intrinsic kernel for the combination of a global geopotential model of degree M with terrestrial gravity data (cf. Vaníček and Sjöberg 1991). Thus, the spheroidal kernel should not be regarded as a modified kernel.

However, this does not preclude the use of a different degree L ($\leq M$) in Eq. (23), which could then be considered as a spheroidally modified kernel (e.g. Wong and Gore 1969).

Using an approach similar to that applied to Eq. (2), the spheroidal Stokes kernel, Eq. (23), is rewritten as

$$\overline{S}^M(\psi,\psi_o)=\begin{cases} S^M(\psi) & \text{for } 0\leq\psi\leq\psi_o \\ 0 & \text{for } \psi_o<\psi\leq\pi \end{cases} \tag{25}$$

or as an infinite Fourier series of Legendre polynomials by

$$\overline{S}^M(\psi,\psi_o)=\sum_{n=2}^{\infty}\frac{2n+1}{2}s_n^M(\psi_o)P_n(\cos\psi) \tag{26}$$

where $s_n^M(\psi_o)$ are coefficients associated with the spheroidal kernel, which will be determined later in this section.

Using the definition in Eq. (25), the spheroidal Stokes integral in conjunction with the geopotential model, Eq. (24), is now given by the following integration over the whole Earth.

$$N_2=N_M+\kappa\int_0^{2\pi}\int_0^{\pi}\overline{S}^M(\psi,\psi_o)\Delta g^M\sin\psi\ \mathrm{d}\psi\ \mathrm{d}\alpha \tag{27}$$

Substituting Eqs. (5) and (26) in Eq. (27), then using the orthogonality relations over the sphere, gives its spectral form as

$$\begin{aligned} N_2=\ & c\sum_{n=2}^{M}\frac{2}{n-1}\Delta g_n^G+c\sum_{n=2}^{M}s_n^M(\psi_o)\Delta g_n^M \\ & +c\sum_{n=M+1}^{\infty}s_n^M(\psi_o)\Delta g_n^M \end{aligned} \tag{28}$$

which is analogous with Eq. (11).

The estimates of the spectral components (surface spherical harmonics) of the gravity anomalies implied by the geopotential model ($\Delta\hat{g}_n^G$) and the terrestrial gravity data ($\Delta\hat{g}_n^T$) are inserted into Eq. (28) to give

$$\begin{aligned} \hat{N}_2=\ & c\sum_{n=2}^{M}\left[\left(\frac{2}{n-1}-s_n^M(\psi_o)\right)\Delta\hat{g}_n^G+s_n^M(\psi_o)\Delta\hat{g}_n^T\right] \\ & +c\sum_{n=M+1}^{\infty}s_n^M(\psi_o)\Delta\hat{g}_n^T \end{aligned} \tag{29}$$

For the spheroidal Stokes integral, Eq. (24), the propagation of errors into the geoid from the terrestrial gravity data and geopotential model are now governed by the coefficients $s_n^M(\psi_o)$. These are therefore derived by rearranging Eq. (26), in conjunction with the orthogonality relations, to give

$$s_n^M(\psi_o)=\int_0^{\pi}\overline{S}^M(\psi,\psi_o)P_n(\cos\psi)\sin\psi\ \mathrm{d}\psi \tag{30}$$

The spheroidal truncation coefficients [cf. Eq. (14)] are defined by Vaníček and Kleusberg (1987) as

$$\begin{aligned} Q_n^M(\psi_o)&=\int_{\psi_o}^{\pi}S^M(\psi)P_n(\cos\psi)\sin\psi\ \mathrm{d}\psi \\ &=Q_n(\psi_o)-\int_{\psi_o}^{\pi}\sum_{k=2}^{M}\frac{2k+1}{k-1}P_k(\cos\psi) \\ &\qquad\times P_n(\cos\psi)\sin\psi\mathrm{d}\psi \end{aligned} \tag{31}$$

The relations given by Eqs. (23), (25) and (31) are then used in Eq. (30) to yield

$$\begin{aligned} s_n^M(\psi_o)=\ & \sum_{n=M+1}^{\infty}\frac{2n+1}{n-1}\int_0^{\pi}[P_n(\cos\psi)]^2\sin\psi\ \mathrm{d}\psi \\ & -Q_n^M(\psi_o) \end{aligned}$$

or

$$s_n^M(\psi_o)=\begin{cases} -Q_n^M(\psi_o) & \text{for } 2\leq n\leq M \\ \frac{2}{n-1}-Q_n^M(\psi_o) & \text{for } M<n<\infty \end{cases} \tag{32}$$

when using the orthogonality relations.

Inserting this result in Eq. (29), together with the degree-errors in the geopotential model-derived gravity anomalies (ϵ_n^G) and terrestrial gravity anomalies (ϵ_n^T), gives

$$\begin{aligned} \hat{N}_2=\ & c\sum_{n=2}^{M}\left[\left(\frac{2}{n-1}+Q_n^M(\psi_o)\right)\{\Delta g_n^G+\epsilon_n^G\}\right. \\ & \left.-Q_n^M(\psi_o)\{\Delta g_n^T+\epsilon_n^T\}\right] \\ & +c\sum_{n=M+1}^{\infty}\left(\frac{2}{n-1}-Q_n^M(\psi_o)\right)\left\{\Delta g_n^T+\epsilon_n^T\right\} \end{aligned} \tag{33}$$

Again, the superscripts G and T are retained to show the origin of the gravity anomalies used. A comparison of Eq. (33) with Eq. (3) indicates the error in the geoid that now occurs when using the spheroidal Stokes integral in conjunction with a global geopotential model [Eq. (24)]. This is

$$\begin{aligned} \epsilon_{N2}=\ & c\sum_{n=2}^{M}\left[\frac{2}{n-1}\epsilon_n^G+Q_n^M(\psi_o)(\epsilon_n^G-\epsilon_n^T)\right] \\ & +c\sum_{n=M+1}^{\infty}\left[\frac{2}{n-1}\epsilon_n^T-Q_n^M(\psi_o)\Delta g_n^T-Q_n^M(\psi_o)\epsilon_n^T\right] \end{aligned} \tag{34}$$

As was done for Eq. (19), Eq. (34) is divided among the error contributions from the geopotential model, the terrestrial gravity data, and the truncated integration domain, respectively, to give

$$\begin{aligned} \epsilon_{N2}=\ & c\sum_{n=2}^{M}\left(\frac{2}{n-1}+Q_n^M(\psi_o)\right)\epsilon_n^G \\ & -c\sum_{n=2}^{M}Q_n^M(\psi_o)\epsilon_n^T+c\sum_{n=M+1}^{\infty}\left(\frac{2}{n-1}-Q_n^M(\psi_o)\right)\epsilon_n^T \\ & -c\sum_{n=M+1}^{\infty}Q_n^M(\psi_o)\Delta g_n^T \end{aligned} \tag{35}$$

Figure 2 shows the numerical values of the coefficients in Eq. (35) that control the propagation of the degree-errors from the geopotential model (ϵ_n^G) and the terrestrial gravity anomalies (ϵ_n^T). All coefficients have been normalised by the $(n-1)/2$ term. Again, the values of $M = 360$ and $\psi_o = 6°$ have been chosen to show a representative case of the coefficients' behaviour, and to allow for a direct comparison with Figs. 1b and 4.

An important point to observe from Fig. 2 is that the numerical values of the $Q_n^M(\psi_o)$ coefficients become unstable in the vicinity of $M = 360$. This is a consequence of the Gibbs phenomenon, where the spherical Stokes kernel is made discontinuous by the removal of the Legendre polynomials. This effect is actually quite small, but has been enhanced by the normalisation of $(n-1)/2$ used purely for the sake of the presentation of the figures.

The truncation error [the last term on the right-hand side of Eq. (35)] must clearly also be considered when the spheroidal Stokes integral, Eq. (24), is used to compute the geoid. However, the impact of this term is reduced because $|Q_n^M(\psi_o)| < |Q_n(\psi_o)|$ for most of the degrees $n > 360$ (cf. Figs. 1b, 2, and also see Fig. 3). Therefore, one of the benefits of using the spheroidal Stokes kernel is that it reduces the magnitude of the truncation error.

There are also other differences between Eqs. (35) and (19), which can be seen by comparing Figs. 1b and 2, as follows.

1. The propagation of errors from the geopotential model (ϵ_n^G) is attenuated less than for the spherical kernel because
$$\left|1 + \frac{n-1}{2} Q_n^M(\psi_o)\right| > \left|\frac{n-1}{2} Q_n(\psi_o)\right|$$
for most degrees in the region $2 \le n < \sim 320$. As such, the errors pass from the geopotential model into the geoid with a greater magnitude for the spheroidal kernel than for the spherical kernel. This provides the rationale for using a low-degree geopotential model when computing the geoid.
2. Conversely, the low- and medium-frequency errors in the terrestrial gravity data are attenuated to a greater extent when using the spheroidal kernel than for the spherical Stokes kernel. This is because
$$\left|\frac{n-1}{2} Q_n^M(\psi_o)\right| < \left|1 - \frac{n-1}{2} Q_n(\psi_o)\right|$$
for most degrees in the region $2 \le n < \sim 320$. As such, the low-frequency errors in the terrestrial gravity data pass into the geoid with a lower magnitude for the spheroidal kernel than for the spherical kernel.

It is argued that this combination offers a preferable scenario because the low-frequency errors in the geopotential model are expected to be smaller in magnitude than those in the terrestrial gravity anomalies. This is because the low-frequency geopotential coefficients are determined from the perturbations of artificial Earth satellites, which are the best source of this information available. On the other hand, terrestrial gravity data suffer from the existence of inconsistencies between vertical datums, systematic errors in geodetic levelling networks used to reduce the gravity observations, and irregular data coverage with some large areas devoid of data. These and other systematic, low-frequency effects on the accuracy of terrestrial gravity anomalies are described in more detail by Heck (1990).

3.1 Special cases of Eq. (35)

As was done for Eq. (19), three special cases of Eq. (35) are considered as follows. When the spheroidal Stokes

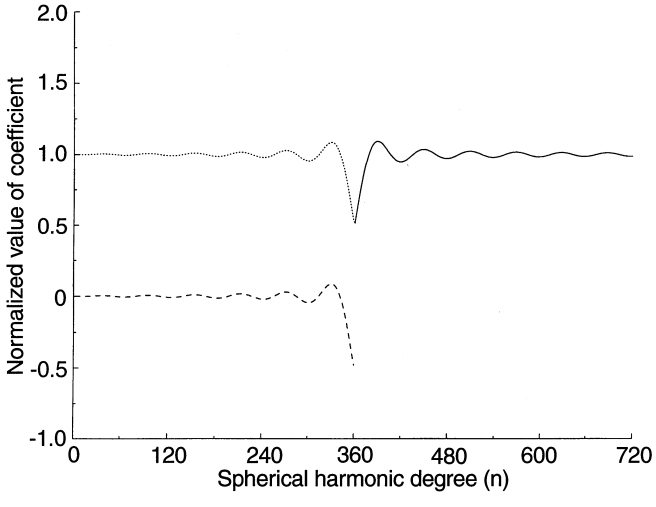

Fig. 2. The normalised spheroidal truncation coefficients $((n-1)/2)Q_n^{360}(6°)$ for $2 \le n \le 360$ (*dashed line*), the sum $\left(1 + ((n-1)/2)Q_n^{360}(6°)\right)$ for $2 \le n \le 360$ (*dotted line*), and the difference $\left(1 - ((n-1)/2)Q_n^{360}(6°)\right)$ for $n > 360$ (*solid line*)

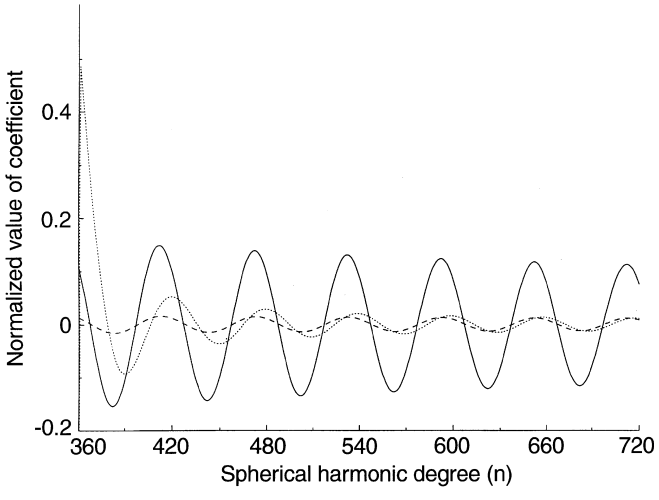

Fig. 3. The normalised truncation coefficients in the region $360 \le n \le 720$ for the spherical Stokes kernel $Q_n(6°)$ (*solid line*), the spheroidal Stokes kernel $Q_n^{360}(6°)$ (*dotted line*) and the $L = 20$ Molodensky-modified spheroidal Stokes kernel $Q_n^{360*}(6°)$ (*dashed line*)

integration is performed over the whole Earth [i.e. $\psi_o = \pi$ in Eq. (24)], the spheroidal truncation coefficients $Q_n^M(\psi_o) = 0,\ \forall n \geq 2$, and Eq. (35) becomes

$$\epsilon_{N2} = c\sum_{n=2}^{M}\frac{2}{n-1}\epsilon_n^G + c\sum_{n=M+1}^{\infty}\frac{2}{n-1}\epsilon_n^T \tag{36}$$

This result shows that the errors in the geopotential model and the terrestrial gravity data both pass undiminished into the geoid, for the low and high frequencies, respectively. When Eq. (36) is compared with Eq. (20), this clearly shows the high-pass filtering property of the spheroidal kernel, where the spheroidal kernel is insensitive to the low frequencies in the terrestrial gravity field. However, this ability of the kernel to completely filter out the low frequencies breaks down when using a spherical cap of limited radius ψ_o due to the presence of the $Q_n^M(\psi_o)$ coefficients in Eq. (35).

As argued earlier, the low-frequency errors in the geopotential model are expected to be smaller than those in the terrestrial gravity anomalies. This provides a clear rationale for the use of at least a low-degree spheroidal Stokes kernel, such that the undesirable effect of low-frequency errors in the terrestrial gravity data on the geoid is suppressed as much as possible.

For the case of no integration [i.e. $\psi_o = 0$ in Eq. (24)], the spheroidal truncation coefficients $Q_n^M(\psi_o) = 0$, $\forall n \geq 2$, and Eq. (35) becomes

$$\epsilon_{N2} = c\sum_{n=2}^{M}\frac{2}{n-1}\epsilon_n^G + c\sum_{n=M+1}^{\infty}\frac{2}{n-1}\Delta g_n^T \tag{37}$$

where the truncation error reaches its maximum value (i.e. it is equal to the omission error of the geopotential model), and the error in the geopotential coefficients again passes undiminished into the geoid. Equation (37) is identical to Eq. (21) and is equivalent to using only the geopotential model to compute the geoid.

When an error-free geopotential model is considered (i.e. $\epsilon_n^G = 0$ for $2 \leq n \leq M$), together with the spheroidal Stokesian integration over a limited spherical cap bound by ψ_o, then Eq. (35) becomes

$$\epsilon_{N2} = c\sum_{n=2}^{M}Q_n^M(\psi_o)\,\epsilon_n^T - c\sum_{n=M+1}^{\infty}\left(\frac{2}{n-1} - Q_n^M(\psi_o)\right)\epsilon_n^T - c\sum_{n=M+1}^{\infty}Q_n^M(\psi_o)\Delta g_n^T \tag{38}$$

In this result, the low-frequency errors in the terrestrial gravity data also leak into the low-frequency geoid. However, their effect is now attenuated by the coefficients $Q_n^M(\psi_o)$. This represents a greater amount of attenuation than for the spherical Stokes integral [cf. Eqs. (38) and (22)] because

$$\left|\frac{n-1}{2}Q_n^M(\psi_o)\right| < \left|1 - \frac{n-1}{2}Q_n(\psi_o)\right|$$

for most degrees in the region $2 \leq n < \sim 320$. This is evident by comparing Figs. 1b and 2, and again illustrates that it is preferable to use a spheroidal Stokes's integral in the presence of low-frequency errors in the terrestrial gravity data (see earlier arguments).

4 The Molodensky-modified spheroidal Stokes kernel

Equation (6) is now used in conjunction with the Molodensky-modified spheroidal Stokes kernel [$S^{M*}(\psi)$] according to the generalised scheme described by Vaníček and Sjöberg (1991), such that

$$N_3 = N_M + \kappa\int_0^{2\pi}\int_0^{\psi_o} S^{M*}(\psi)\Delta g^M \sin\psi\ \mathrm{d}\psi\ \mathrm{d}\alpha \tag{39}$$

where $S^{M*}(\psi)$ is the Molodensky-modified spheroidal Stokes kernel given by Vaníček and Kleusberg (1987). This type of kernel modification was designed specifically to reduce the upper bound of the truncation error in a least-squares sense (Vaníček and Sjöberg 1991).

The degree of modification to the kernel (L) can be less or equal to the degree of spheroid used (M). However, it can never be greater than the degree of the spheroid, since this violates the boundary value problem and thus requires the inclusion of an additional term. This term will not be discussed in this paper. Therefore, the degree of modification ($L \leq M$) is introduced to give

$$S^{M*}(\psi) = S^M(\psi) - \sum_{k=2}^{L}\frac{2k+1}{2}t_k(\psi_o)P_k(\cos\psi) \tag{40}$$

where $t_k(\psi_o)$ are the coefficients that are used to apply the spheroidal Molodensky modification. These are determined for $2 \leq n \leq L$ using the following linear system of equations (Vaníček and Kleusberg 1987):

$$\sum_{k=2}^{L}\frac{2k+1}{2}t_k(\psi_o)e_{nk}(\psi_o) = Q_n^L(\psi_o) = Q_n(\psi_o) - \sum_{k=2}^{L}\frac{2k+1}{k-1}e_{nk}(\psi_o) \tag{41}$$

where the coefficients

$$e_{nk}(\psi_o) = \int_{\psi_o}^{\pi}P_n(\cos\psi)P_k(\cos\psi)\sin\psi\ \mathrm{d}\psi \tag{42}$$

Also note that in the region $2 \leq n \leq L$, Eq. (41) is equal to Eq. (31). It is therefore acknowledged that the expression for the $t_k(\psi_o)$ coefficients shown by Vaníček and Sjöberg (1991) has a typographical error in the denominator, where 2 is used instead of $(k-1)$. However, the definition derived herein and the original definition shown in Vaníček and Kleusberg (1987) are correct.

As for the previous two implementations of Stokes's integral, the Molodensky-modified spheroidal Stokes kernel in Eq. (40) is rewritten as

$$\overline{S}^{M*}(\psi,\psi_o)=\begin{cases} S^{M*}(\psi) & \text{for } 0\le\psi\le\psi_o \\ 0 & \text{for } \psi_o<\psi\le\pi \end{cases} \tag{43}$$

and the corresponding Fourier series of Legendre polynomials is

$$\overline{S}^{M*}(\psi,\psi_o)=\sum_{n=2}^{\infty}\frac{2n+1}{2}s_n^{M*}(\psi_o)P_n(\cos\psi) \tag{44}$$

where s_n^{M*} are the coefficients associated with this modified kernel, and will be defined later in this section.

Using the same procedures as for the spherical and spheroidal Stokes kernels, Eq. (39) is transformed to a spectral form, then the estimates of the gravity anomalies as implied by the geopotential model ($\Delta\hat{g}_n^G$) and terrestrial gravity data ($\Delta\hat{g}_n^T$) are inserted, to give

$$\begin{aligned}\hat{N}_3=c\sum_{n=2}^{M}\Bigg[\left(\frac{2}{n-1}-s_n^{M*}(\psi_o)\right)\Delta\hat{g}_n^G \\ +s_n^{M*}(\psi_o)\Delta\hat{g}_n^T\Bigg] \\ +c\sum_{n=M+1}^{\infty}s_n^{M*}(\psi_o)\Delta\hat{g}_n^T\end{aligned} \tag{45}$$

Equation (45) shows that the propagation of errors through Eq. (39) is now controlled by the coefficients $s_n^{M*}(\psi_o)$. Therefore, these coefficients are derived by rearranging Eq. (40) in conjunction with the orthogonality relations to give

$$s_n^{M*}(\psi_o)=\int_0^{\pi}\overline{S}^{M*}(\psi,\psi_o)P_n(\cos\psi)\sin\psi\,\mathrm{d}\psi \tag{46}$$

The Molodensky-modified spheroidal truncation coefficients [$Q_n^{M*}(\psi_o)$] are defined by Vaníček and Kleusberg (1987) as

$$Q_n^{M*}(\psi_o)=\int_{\psi_o}^{\pi}S^{M*}(\psi)P_n(\cos\psi)\sin\psi\,\mathrm{d}\psi \tag{47}$$

[cf. Eqs. (14) and (31)]. Inserting Eqs. (47) and (43) in Eq. (46) gives

$$s_n^{M*}(\psi_o)=\int_0^{\pi}S^{M*}(\psi)P_n(\cos\psi)\sin\psi\,\mathrm{d}\psi-Q_n^{M*}(\psi_o) \tag{48}$$

Then, substituting Eq. (40) for the Molodensky-modified Stokes kernel, recalling that $L\le M$, gives

$$\begin{aligned}s_n^{M*}(\psi_o)=\int_0^{\pi}S^{M}(\psi)P_n(\cos\psi)\sin\psi\,\mathrm{d}\psi \\ -\sum_{k=2}^{M}\frac{2k+1}{2}\int_0^{\pi}t_k(\psi_0)P_k(\cos\psi)P_n(\cos\psi) \\ \times\sin\psi\,\mathrm{d}\psi \\ -Q_n^{M*}(\psi_o)\end{aligned} \tag{49}$$

Using the definition in Eq. (23) and the orthogonality relations to replace the integral terms in Eq. (49), then separating the low- ($2\le n\le L$), medium- ($L<n\le M$) and high-frequency ($M\le n<\infty$) components, gives

$$s_n^{M*}(\psi_o)=\begin{cases} -t_n(\psi_o)-Q_n^{M*}(\psi_o) & \text{for } 2\le n\le L \\ -Q_n^{M*}(\psi_o) & \text{for } L<n\le M \\ \frac{2}{n-1}-Q_n^{M*}(\psi_o) & \text{for } M<n<\infty \end{cases} \tag{50}$$

By definition, the Molodensky-modified spheroidal truncation coefficients $Q_n^{M*}(\psi_o)$ are zero in the region $2\le n\le L$ [cf. Eqs. (41) and (47) herein, or Eqs. (38) and (22) of Vaníček and Sjöberg (1991)]. Therefore, the $s_n^{M*}(\psi_o)$ coefficients are given by

$$s_n^{M*}(\psi_o)=\begin{cases} -t_n(\psi_o) & \text{for } 2\le n\le L \\ -Q_n^{M*}(\psi_o) & \text{for } L<n\le M \\ \frac{2}{n-1}-Q_n^{M*}(\psi_o) & \text{for } M<n<\infty \end{cases} \tag{51}$$

Using this result and dividing the contribution among the three frequency bands, Eq. (45) becomes

$$\begin{aligned}\hat{N}_3=c\sum_{n=2}^{L}\left[\left(\frac{2}{n-1}+t_n(\psi_o)\right)\Delta\hat{g}_n^G-t_n(\psi_o)\Delta\hat{g}_n^T\right] \\ +c\sum_{n=L+1}^{M}\left[\left(\frac{2}{n-1}+Q_n^{M*}(\psi_o)\right)\Delta\hat{g}_n^G-Q_n^{M*}(\psi_o)\Delta\hat{g}_n^T\right] \\ +c\sum_{n=M+1}^{\infty}\left(\frac{2}{n-1}-Q_n^{M*}\right)\Delta\hat{g}_n^T\end{aligned} \tag{52}$$

Next, the degree-errors in the geopotential model-derived gravity anomalies (ϵ_n^G) and the terrestrial gravity anomalies (ϵ_n^T) are introduced into Eq. (52), the terms expanded, and Eq. (3) subtracted. As before, the error is then divided among the contribution from the geopotential model, the terrestrial gravity data and the truncation error. This leaves the error in the geoid that occurs when using the Molodensky-modified spheroidal Stokes formula [Eq. (39)] as

$$\begin{aligned}\epsilon_{N3}=c\sum_{n=2}^{L}\left(\frac{2}{n-1}+t_n(\psi_o)\right)\epsilon_n^G \\ +c\sum_{n=L+1}^{M}\left(\frac{2}{n-1}+Q_n^{M*}(\psi_o)\right)\epsilon_n^G \\ -c\sum_{n=2}^{L}t_n(\psi_o)\epsilon_n^T-c\sum_{n=L+1}^{M}Q_n^{M*}(\psi_o)\epsilon_n^T \\ +c\sum_{n=M+1}^{\infty}\left(\frac{2}{n-1}-Q_n^{M*}(\psi_o)\right)\epsilon_n^T \\ -c\sum_{n=M+1}^{\infty}Q_n^{M*}(\psi_o)\Delta g_n^T\end{aligned} \tag{53}$$

The last term on the right-hand side of Eq. (53) comprises the truncation error. Its impact has been minimised by Vaníček and Kleusberg (1987) according to the Molodensky et al. (1962) argument. This is because $|Q_n^{M*}(\psi_o)| < |Q_n^M(\psi_o)| < |Q_n(\psi_o)|$ for most of the degrees $n > \sim 400$ (see Fig. 3), and is supported further by the numerical results shown later in Table 1.

Figure 4 shows the behaviour of the coefficients that control the error propagation when using the Molodensky-modified spheroidal Stokes kernel [Eq. (40)]. The values of $\psi_o = 6^\circ$ and $M = 360$ have been used for consistency, and the value of $L = 20$ has been used for the degree of Molodensky modification. The rationale for this degree of kernel modification has already been given by Vaníček and Kleusberg (1987), and will not be duplicated here. Theoretically, however, it does not matter what degree of kernel modification is used to produce Fig. 4, provided that L is never greater than M.

From Fig. 4, the low-frequency ($2 \le n \le 20$) errors in the geopotential model (ϵ_n^G) now pass into the geoid with a slightly greater magnitude than for the spherical kernel because

$$\left|1 + \frac{n-1}{2} t_n(\psi_o)\right| > \left|\frac{n-1}{2} Q_n(\psi_o)\right|$$

(cf. Figs. 1b and 4 for $2 \le n \le 20$). Conversely, the amount of error propagation is less than that associated with the spheroidal Stokes kernel because

$$\left|1 + \frac{n-1}{2} t_n(\psi_o)\right| < \left|1 - \frac{n-1}{2} Q_n(\psi_o)\right|$$

(cf. Figs. 2 and 4 for some of the degrees in the region $2 \le n \le 20$). Based on the earlier arguments, this is not critical because the geopotential model is currently always the best source of low-frequency gravity field information.

Also from Fig. 4, the very low-frequency terrestrial gravity data errors are also attenuated more when using the Molodensky-modified spheroidal kernel compared to the spherical Stokes kernel. This is because

$$\left|\frac{n-1}{2} t_n(\psi_o)\right| < \left|1 - \frac{n-1}{2} Q_n(\psi_o)\right|$$

(cf. Figs. 1b and 4 for $2 \le n \le 20$). However, the amount of attenuation is not as great as that for the spheroidal Stokes kernel, because $|t_n(\psi_o)| > |Q_n(\psi_o)|$ (cf. Figs. 2 and 4 for $2 \le n \le M$). This is a direct consequence of minimising the truncation error using the Molodensky approach, and allows for more leakage of very low-frequency terrestrial gravity data errors into the geoid. Nevertheless, the amount of leakage is still much less than that associated with the spherical Stokes kernel.

Next, it is interesting to see what effect the $L = 20$ Molodensky modification has on the medium frequencies ($2 \le n \le 360$) in the geopotential model and the terrestrial gravity data. Compared to the spherical kernel, the Molodensky-modified spheroidal kernel attenuates more of the geopotential model error. This is because

$$\left|\frac{n-1}{2} Q_n^{M*}(\psi_o)\right| < \left|1 - \frac{n-1}{2} Q_n(\psi_o)\right|$$

(cf. Figs. 1b, 4). Similarly, the Molodensky-modified spheroidal kernel attenuates more of the geopotential model error because

$$\left|\frac{n-1}{2} Q_n^{M*}(\psi_o)\right| < \left|1 + \frac{n-1}{2} Q_n^M(\psi_o)\right|$$

(cf. Figs. 2, 4).

When considering the propagation of medium-frequency terrestrial gravity data errors ($21 \le n \le 360$), the Molodensky-modified spheroidal kernel attenuates more error than the spherical Stokes kernel. This can be seen by comparing Figs. 1b and 4. Conversely, the Molodensky-modified spheroidal kernel attenuates less error than the spheroidal Stokes kernel, because $|Q_n^{M*}(\psi_o)| > |Q_n^M(\psi_o)|$ for most degrees in the region $21 \le n < \sim 320$ that is unaffected by the Gibbs phenomenon in the spheroidal kernel (cf. Figs. 2, 4). A numerical comparison of these effects will be given later in the paper, that supports the statements made here.

Another interesting point is that the Molodensky-modified spheroidal kernel is less affected by the Gibbs phenomenon about $M = 360$. This is because the application of the modification makes the kernel a more continuous function that is very much less sensitive to this effect.

4.1 Special cases of Eq. (52)

When integration of Eq. (39) is performed over the whole Earth (i.e. $\psi_o = \pi$), the coefficients $t_n(\psi_o) = Q_n^{M*}(\psi_o) = 0$, $\forall n \ge 2$. Thus, Eq. (53) becomes

$$\epsilon_{N3} = c \sum_{n=2}^{M} \frac{2}{n-1} \epsilon_n^G + c \sum_{n=M+1}^{\infty} \frac{2}{n-1} \epsilon_n^T \tag{54}$$

which is an identical result to Eq. (36), where the errors in the geopotential model and terrestrial gravity data pass undiminished into the geoid. Based on the earlier arguments that $|\epsilon_n^T| > |\epsilon_n^G|$ for the very low frequencies, it is thus preferable to use a low-degree geopotential model to provide the low-frequency component of the geoid.

In the case of no integration [i.e. $\psi_o = 0$ in Eq. (39)], $t_n(\psi_o) = Q_n^{M*}(\psi_o) = \frac{2}{n-1}$, $\forall n \ge 2$. This yields the same result as Eqs. (21) and (37), specifically

$$\epsilon_{N3} = c \sum_{n=2}^{M} \frac{2}{n-1} \epsilon_n^G + c \sum_{n=M+1}^{\infty} \frac{2}{n-1} \Delta g_n^T \tag{55}$$

Again, this is equivalent to using only the geopotential model to compute the geoid. Therefore, if the integration is not used in each of the three cases discussed, it becomes immaterial just what form of kernel is used. The second term on the right-hand side of Eq. (55) is the truncation error, which is identical to the omission error of the geopotential model.

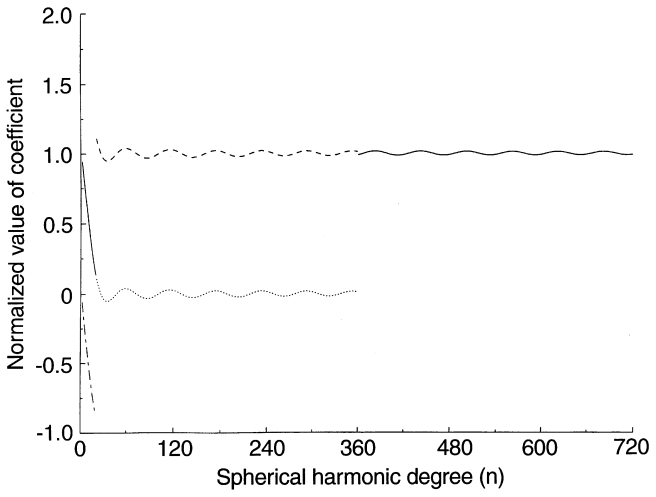

Fig. 4. The normalised Molodensky-modification coefficients $t_n(6°)$ for $2 \le n \le 20$ (*dot–dashed line*), the sum $(1 + ((n-1)/2)t_n(6°))$ for $2 < n \le 20$ (*solid line*), the normalised Molodensky-modification coefficients $t_n(6°)$ for $21 \le n \le 360$ (*dotted line*), the sum $\left(1 + ((n-1)/2)Q_n^{20*}(6°)\right)$ for $21 \le n \le 360$ (*dashed line*), and the difference $\left(1 - n - 1/2Q_n^{20*}(6^o)\right)$ for $n > 360$ (*solid line*)

When using an error-free geopotential model (i.e. $\epsilon_n^G = 0$ for $2 \le n \le M$), and integration over a limited spherical cap, the error in the geoid is contaminated by the terrestrial gravity data errors in both the high and low frequencies. This is given by

$$\begin{aligned}\epsilon_{N3} = &- c\sum_{n=2}^{L} t_n(\psi_o)\epsilon_n^T - c\sum_{n=L+1}^{M} Q_n^{M*}(\psi_o)\epsilon_n^T \\ &+ c\sum_{n=M+1}^{\infty}\left(\frac{2}{n-1} - Q_n^{M*}(\psi_o)\right)\epsilon_n^T \\ &- c\sum_{n=M+1}^{\infty} Q_n^{M*}(\psi_o)\Delta g_n^T\end{aligned} \tag{56}$$

In this special case, the very low-frequency errors in the terrestrial gravity data are attenuated to a greater extent than for the spherical Stokes formula because

$$\left|\frac{n-1}{2}t_n(\psi_o)\right| < \left|1 - \frac{n-1}{2}Q_n(\psi_o)\right|$$

(cf. Figs. 1b and 4 for $2 \le n \le 20$). However, the amount of error attenuation is less than that experienced with the spheroidal Stokes integral because $|t_n(\psi_o)| > |Q_n^M(\psi_o)|$ (cf. Figs. 2 and 4 for $2 \le n \le 20$). As stated, this is a consequence of minimising the truncation error.

In the medium frequencies, the terrestrial gravity data errors are attenuated more by the Molodensky-modified spheroidal kernel than for the spherical or spheroidal kernels. For the spherical kernel, this is because

$$\left|\frac{n-1}{2}Q_n^{M*}(\psi_o)\right| < \left|1 - \frac{n-1}{2}Q_n(\psi_o)\right|$$

(cf. Figs. 1b and 4 for $21 \le n \le 360$). For the spheroidal kernel, this is because

$$\left|\frac{n-1}{2}Q_n^{M*}(\psi_o)\right| < \left|1 + \frac{n-1}{2}Q_n^{M}(\psi_o)\right|$$

(cf. Figs. 2 and 4 for $21 \le n < 360$). This result is a beneficial by-product of the Molodensky modification, which was designed specifically to minimise the truncation error and hence $Q_n^{M*}(\psi_o)$.

5 How do terrestrial gravity data improve the geopotential model?

Now that the mathematical descriptors have been derived for the propagation of errors from the geopotential model (ϵ_n^G) and terrestrial gravity data (ϵ_n^T) into the geoid, the question originally posed in this paper can be addressed. Specifically, the claim that the terrestrial gravity data (Δg^T) attenuate errors present in the geopotential model, and to what extent this is true for each of the three kernels, will be considered. An empirical estimation of this effect has already been considered by Sideris and Schwarz (1987) for the spherical Stokes kernel, but it is important to know how this compares with other implementations of Stokes kernel.

5.1 An error-free terrestrial gravity field

First, the performance of the three kernels is now investigated using the special case of an error-free terrestrial gravity field (i.e. $\epsilon_n^T = 0$ for $2 \le n \le M$). The truncation error term will be ignored, which is justified because this only affects the high-frequency geoid and thus gives no answer to the question in hand. Nevertheless, the influence of the truncation error is reduced by both the spheroidal and Molodensky-modified kernels, as shown in Fig. 3, and this will be discussed further in the next section.

Inserting the above conditions in Eq. (19) gives the error originating from the geopotential model that remains in the geoid when computed by means of the spherical Stokes function. This is

$$\epsilon_{N1} = c\sum_{n=2}^{M} Q_n(\psi_o)\epsilon_n^G \tag{57}$$

Equation (57) clearly shows that even error-free terrestrial gravity data, when used in a cap, can never completely correct the errors present in the geopotential model. This is due to the presence of the spherical truncation coefficients $Q_n(\psi_o)$. If terrestrial gravity data were to completely correct the geopotential model, then the $Q_n(\psi_o)$ coefficients would have to be zero in the region $2 \le n \le M$. This is clearly not the case, as shown in Fig. 1, except for the points at which the coefficient curve passes through zero. The $Q_n(\psi_o)$ coefficients will only become zero $\forall n$ if and only if $\psi_o = \pi$ (i.e. an integration over the whole Earth). Moreover, the smaller the radius of integration (ψ_o), the larger the magnitude of the spherical truncation coefficients, and thus the less the terrestrial

data can begin to account for any error in the geopotential model.

When an error-free terrestrial gravity field is used in Eq. (35), and the truncation error neglected, the error originating in the geopotential model and remaining in the geoid when computed by the spheroidal Stokes kernel is given by

$$\epsilon_{N2} = c \sum_{n=2}^{M} \left(\frac{2}{n-1} + Q_n^M(\psi_o) \right) \epsilon_n^G \tag{58}$$

Once again, Eq. (58) shows that the terrestrial gravity data, when used in a cap, cannot completely correct the low-frequency errors in the geopotential model. In this case, the errors generated by the geopotential model remain, almost unaltered, in the geoid because the coefficients $Q_n^M(\psi_o) << 2/(n-1)$ (see Fig. 2 for $2 \leq n < \sim 320$). In fact, the errors are diminished more effectively close to $M = 360$ courtesy of the Gibbs phenomenon. However, this must be balanced against the effect that the Gibbs phenomenon will have on the propagation of the gravity signal into the geoid.

Equation (58) also illustrates the (partial) high-pass filtering property of the spheroidal Stokes kernel, where the contribution of the terrestrial gravity data to the geoid is attenuated according to the coefficients $(2/(n-1) + Q_n^M(\psi_o))$. If the terrestrial gravity data were to completely correct the geopotential model, then the $Q_n^M(\psi_o)$ coefficients would have to be equal to $-2/(n-1)$, which again can only be satisfied by a global integration.

When using an error-free terrestrial gravity field in the Molodensky-modified spheroidal Stokes integral, (Eq. 40), and again neglecting the truncation error, the geoid error originating from the geopotential model, Eq. (53), becomes

$$\begin{aligned} \epsilon_{N3} = {} & c \sum_{n=2}^{L} \left(\frac{2}{n-1} + t_n(\psi_o) \right) \epsilon_n^G \\ & + c \sum_{n=L+1}^{M} \left(\frac{2}{n-1} + Q_n^{M*}(\psi_o) \right) \epsilon_n^G \end{aligned} \tag{59}$$

Equation (59) also shows that the terrestrial gravity data from within a cap cannot completely correct the low-frequency errors in the geopotential model. In this case, the error in the geoid propagating from the geopotential model is diminished more than for the spheroidal Stokes kernel, because $|t_n(\psi_o)| < |Q_n^M(\psi_o)|$ (cf. Figs. 2 and 3 for $2 \leq n \leq 20$) and $|Q_n^{M*}(\psi_o)| < |Q_n^M(\psi_o)|$ (cf. Figs. 2 and 3 for $21 \leq n \sim 320$). The same arguments apply to the spherical kernel. Once again, this illustrates that the Molodensky-modified spheroidal Stokes kernel attenuates the low frequencies in the terrestrial gravity data. However, the high-pass filter is imperfect and some low-frequency errors leak into the low frequencies of the geoid. This is a price that must be paid for the minimisation of the truncation error.

It is clear from these three very special cases that even error-free terrestrial gravity data *cannot* correct the errors in a geopotential model. This applies when they are used within a limited spherical cap surrounding the geoid computation point, due to the truncated integration. However, given that the low-frequency errors in the terrestrial gravity data are expected to be larger than the low-frequency errors in the geopotential model, this raises some question as to the appropriateness of using the spherical Stokes kernel in Eq. (6). In the presence of low-frequency terrestrial gravity data errors, it is therefore preferable to use one of the spheroidal kernels because they can attenuate a larger amount of these errors.

5.2 *Numerical comparisons of the kernel filtering properties*

Next, it is informative to quantify just how effective each form of Stokes's kernel is at correcting the errors in the geopotential model. In order to answer this question properly, the error characteristics of each of the two sources of information (i.e. ϵ_n^G for the geopotential model and ϵ_n^T for the terrestrial gravity data) would have to be known. Unfortunately, however, ϵ_n^T are largely unknown for the terrestrial data. Of course, some error characteristics could be postulated, but any such postulation would be speculative and subject to criticism and maybe even controversy. Instead, a less controversial approach is taken whereby the $M = 360$ geopotential model is divided into three frequency bands, as follows.

1. Spherical harmonic degrees $2 \leq n \leq 20$, for which the geopotential model is considered to be the best source of gravity field information (because of the satellite-derived contribution) and the terrestrial data are a much poorer source of this information (for the reasons explained earlier).
2. Spherical harmonic degrees $20 < n \leq 120$, for which the geopotential model gives a reasonable accuracy almost everywhere on Earth, and where the terrestrial data may offer an improvement in certain parts of the world, only if these data are of good quality.
3. Spherical harmonic degrees $120 < n \leq 360$, for which the geopotential model may not be the best source of gravity field information, and an improvement from terrestrial data should thus be sought. The degradation of the geopotential model in this region can be seen from the error degree variances which are usually greater than 50% of the signal strength.

The performance of each of the three kernels discussed here is investigated separately for each of the above frequency bands. However, an appropriate measure of the relative performance of each kernel must be devised. Firstly, the following general criteria should be satisfied.

(a) The total contribution of all errors should be as small as possible,
(b) Whatever the errors in the geopotential model may be, how much of the error in the terrestrial gravity data is going to leak into the combined solution,
(c) Conversely, whatever the errors are in the terrestrial gravity data may be, how much of the error in the

geopotential model is going to remain in the combined solution.

Given this, the question "to what extent can terrestrial gravity data correct errors in a high-degree geopotential model?" should be posed in terms that can more readily be translated into mathematical expressions. Therefore, the question is rephrased as "which kernel gives the least ϵ_N and the best balance between ϵ_n^G and ϵ_n^T for the $2 \le n \le 360$ contribution to ϵ_N?". This formulation automatically eliminates the truncation error from the following deliberations. It also obviates the investigation of the effect of ϵ_n^T for $n > 360$. Nevertheless, the truncation error will be briefly discussed at the end of this section.

A plausible way of measuring the contribution of the terrestrial data errors (ϵ_n^T) and geopotential model errors (ϵ_n^G) is now devised, given that these errors are not actually known. The error (ϵ_N^*) in the first $M = 360$ terms of the combined geoid can be written as

$$\begin{aligned}\epsilon_N^* &= c\sum_{n=2}^{M} f_n^G \epsilon_n^G + c\sum_{n=2}^{M} f_n^T \epsilon_n^T \\ &= c\langle \mathbf{f}^G, \epsilon^G \rangle + c\langle \mathbf{f}^T, \epsilon^T \rangle\end{aligned} \tag{60}$$

where $\mathbf{f}$ is the vector of filter values f_n which multiplies the vector of the (unknown) error values ϵ_n in either the terrestrial data (T) or geopotential model (G), and $\langle , \rangle$ denotes a scalar product in the space $\mathbf{F}$ of real functions defined for integer arguments in the region $2 \le n \le M$ (i.e. $\mathbf{F} \in \{(2, \ldots, M) \to \Re\}$). The values of the filters $\mathbf{f}^G$ and $\mathbf{f}^T$ for the three kernels under discussion are simply those derived in Eqs. (19), (35) and (53). Not only are these filter vectors different for different n, but also they are different for the three integration kernels. This will be shown later.

Next, the relative contributions of the two scalar products in Eq. (60) are measured for each of the three frequency bands (1 to 3 above). Each band can be thought of as corresponding to three different spaces in $\mathbf{F}$. These are $\mathbf{F}_1 \in \{(2, \ldots, 20) \to \Re\}$, $\mathbf{F}_2 \in \{(21, \ldots, 120) \to \Re\}$ and $\mathbf{F}_3 \in \{(121, \ldots, 360) \to \Re\}$. Consequently, the relative contributions are measured separately in each space as follows. First, the Schwarz inequality

$$\langle a, b \rangle \le \|a\| \, \|b\| \tag{61}$$

is used to give the upper bound for the scalar product. Using the notation given earlier for the filter and error vectors yields

$$\langle \mathbf{f}, \epsilon \rangle \le \|\mathbf{f}\| \, \|\epsilon\| \tag{62}$$

Therefore, for an arbitrary vector (ϵ) of errors (whether they reside in the geopotential model or terrestrial gravity data), the upper bound of its contribution to the geoid is measured by the value of the norm $\|\mathbf{f}\|$. Taking this approach allows for an objective assessment of the filtering properties of each kernel, since the errors in each data source (whatever they may be) will be common to each estimation of the geoid.

The norm adopted in this study is the Euclidean norm, which is given by the following expression:

$$\|\mathbf{f}\| = \sqrt{\sum_{n=i}^{j} f_n^2} \tag{63}$$

where the summation is taken over the $j - i$ spherical harmonic degrees within each space. Specifically, for $\mathbf{F}_1, i = 2$ and $j = 20$, for $\mathbf{F}_2, i = 21$ and $j = 120$, and for $\mathbf{F}_3, i = 121$ and $j = 360$. Other choices of norm are, of course, available.

In order to be able to compare the adopted norms among the three spaces ($\mathbf{F}_1$, $\mathbf{F}_2$ and $\mathbf{F}_3$), Eq. (63) should be standardised by $j - i$ (the dimension of each space). This gives

$$\|\mathbf{f}\|^* = \frac{1}{j-i}\sqrt{\sum_{n=i}^{j} f_n^2} \tag{64}$$

An alternative way of interpreting the standardised norm in Eq. (64) is that it gives the average value of the upper bound of the degree contribution between i and j when multiplied by a degree-error (i.e. ϵ_n^T or ϵ_n^G for $i \le n \le j$).

Next, the expressions for the individual filter values are recalled for the three kernels. For the spherical Stokes kernel, Eq. (57) yields

$$\begin{aligned}\forall n = 2, \ldots, M: \quad f_n^G &= Q_n(\psi_o), \\ f_n^T &= \left(\frac{2}{n-1} - Q_n(\psi_o)\right)\end{aligned} \tag{65}$$

For the spheroidal Stokes kernel, Eq. (35) yields

$$\begin{aligned}\forall n = 2, \ldots, M: \quad f_n^G &= \left(\frac{2}{n-1} + Q_n^M(\psi_o)\right), \\ f_n^T &= -Q_n^M(\psi_o)\end{aligned} \tag{66}$$

For the Molodensky-modified spheroidal Stokes kernel, Eq. (53) yields

$$\begin{aligned}\forall n = 2, \ldots, L: \quad f_n^G &= \left(\frac{2}{n-1} + t_n(\psi_o)\right), \\ f_n^T &= -t_n(\psi_o)\end{aligned}$$

$$\begin{aligned}\forall n = L, .., M: \quad f_n^G &= \left(\frac{2}{n-1} + Q_n^{M*}(\psi_o)\right), \\ f_n^T &= -Q_n^{M*}(\psi_o)\end{aligned} \tag{67}$$

The filter definitions in Eqs. (65), (66) and (67) are then used in Eq. (64) to compute the standardised norms for each space. These are shown in Table 1 for the values of $M = 360$, $L = 20$ and $\psi_o = 6^\circ$.

Obviously, the most desirable performance of a kernel would be to have all three norms equal to zero for both the terrestrial and geopotential data errors. This is impossible to achieve when using terrestrial gravity data in a cap, but should be borne in mind when judging the

relative performance of the three kernels. Therefore, a kernel that is deemed to behave well is one that has the smallest relative value where the input data are expected to contain the largest errors.

The numerical results in Table 1 are now used to consider the relative performance of each kernel in each space in view of the three criteria (a, b and c) set out above.

1. For the space $\mathbf{F}_1$ (spherical harmonic degrees $2 \leq n \leq 20$), the spheroidal kernel appears to perform the best because it filters out the long-wavelength error contribution from the terrestrial data ($||\mathbf{f}^T||_1^* = 3.69 \times 10^{-4}$), whereas the spherical kernel performs the worst ($||\mathbf{f}^T||_1^* = 2.10 \times 10^{-1}$). Recall that a large amount of low-frequency filtering of the terrestrial data is considered to be a desirable feature due to the expected presence of larger errors in this band.

On the other hand, the spherical kernel ($||\mathbf{f}^G||_1^* = 4.58 \times 10^{-1}$) reduces the existing long wavelength errors in the geopotential model marginally better than for the modified spheroidal kernel ($||\mathbf{f}^G||_1^* = 5.79 \times 10^{-1}$), with the spheroidal kernel performing the worst ($||\mathbf{f}^G||_1^* = 5.15 \times 10^{-1}$). However, this consideration is less critical since the geopotential model is the best source of this information in this band. Therefore, considering this and the earlier arguments of the error spectra, the modified spheroidal kernel is judged to perform the best overall.

2. For the space $\mathbf{F}_2$ ($21 \leq n \leq 120$), it is assumed that the errors from both sources are roughly equal. Given this, both the spheroidal and modified spheroidal kernels are judged to be performing worse than the spherical kernel. This is because they filter out less errors in the geopotential model than the spherical kernel, whilst at the same time filtering out more errors in the terrestrial data.

However, the relative merits of the three kernels in this band can only ever be decided upon when the relative errors in the two data sources are known in a particular region. For instance, in areas where the terrestrial data are good, the spherical kernel is preferable and, conversely, where the data are poor. However, this becomes a circular argument for a combined geopotential model since the model is also expected to have similar errors to the data used in its computation. It also leads to the unpleasant correlations between the errors of the terrestrial data which are used in the contributions from the geopotential model and terrestrial data.

3. For the space $\mathbf{F}_3$ ($121 \leq n \leq 360$), the spherical kernel filters out the errors in the geopotential model better than the other two kernels. On the other hand, the spheroidal and modified spheroidal kernels filter out the errors in the terrestrial data better than the spherical kernel. This leads to the question of how these two perspectives be reconciled.

In order to do this, Table 1 is now viewed from the perspective of the overall performance of the three kernels. Most importantly, the error contributions from each band have a progressively smaller effect on the geoid for increasing degree. This is by virtue of the relation in Eq. (3), where most of the geoid's power is contained in the low frequencies, so errors in these frequencies will have the most dramatic effect on the accuracy of the geoid. This indicates that more weight should be placed upon the interpretation of the low-frequency band, and less should be placed upon the high-frequency band. All kernels yield quite reasonable results in the high-frequency band as far as the magnitude of errors that each will allow into the geoid solution is concerned. Therefore, their relative performance should not be interpreted with the same weight as in the low-frequency band.

Table 1. The numerical values of the standardised norms calculated for the three spaces using Eqs. (65), (66) and (67) with $L = 20, M = 360$ and $\psi_o = 6^\circ$ where appropriate

	Spherical	Spheroidal	Molodensky spheroidal
$\|\|\mathbf{f}^G\|\|_1^*$	4.58×10^{-1}	5.79×10^{-1}	5.15×10^{-1}
$\|\|\mathbf{f}^T\|\|_1^*$	2.10×10^{-1}	3.69×10^{-4}	1.04×10^{-1}
$\|\|\mathbf{f}^G\|\|_2^*$	1.58×10^{-2}	4.17×10^{-2}	4.19×10^{-2}
$\|\|\mathbf{f}^T\|\|_2^*$	5.12×10^{-2}	1.26×10^{-4}	1.90×10^{-3}
$\|\|\mathbf{f}^G\|\|_3^*$	1.46×10^{-3}	9.64×10^{-3}	9.66×10^{-3}
$\|\|\mathbf{f}^T\|\|_3^*$	9.95×10^{-3}	4.47×10^{-3}	1.52×10^{-4}

To summarise, the modified spheroidal kernel is judged to be performing the best when considering the above argument and the three criteria (a, b and c) outlined earlier.

5.2.1 The truncation error

In addition to the more desirable high-pass filtering performance of the Molodensky-modified spheroidal Stokes kernel, there is the additional advantage of its reduction of the truncation error. It should be pointed out that this kernel was designed to reduce the truncation error, and its preferable filtering properties are a discovery of this paper. Although the size of the truncation error (synonymously called the far-zone contribution) has not been considered in this paper, it may well be a more important criterion than the filtering properties investigated. Therefore, for the sake of interest, the standardised norm has been computed for the truncation error using

$$||\mathbf{f}||_4^* = \frac{1}{359}\sqrt{\sum_{n=361}^{720} q_n^2} \tag{68}$$

where q_n denotes the respective truncation coefficients shown in Eqs. (19), (35) and (53). As in the case of the errors, these norms can be multiplied by the norm of the high-frequency gravity anomalies (i.e. $||\Delta g^M||$ for $360 < n < \infty$. The series in Eq. (68) has been limited to spherical harmonic degree 720 because the relative contributions remain the same for a further summation. Equation (68) is, therefore, used in the region $360 < n \leq 720$ to show how effective each kernal is at reducing the truncation error. The results are given in Table 2.

From the results in Table 2, it is clear that the Molodensky-modified spheroidal Stokes kernel satisfies its objective of reducing the truncation error. This can also

be seen in Fig. 3, which shows the relative size of the truncation coefficients. In Table 2, the smaller number for the modified spheroidal kernel in relation to the spherical and spheroidal kernels shows that the contribution of the high-frequency gravity anomalies in the remote zones outside the integration cap is indeed reduced by one order of magnitude.

Table 2. The values of the standardised norms calculated for the truncation error using Eqs. (28), (35) and (53) with $L = 20$, $M = 360$ and $\psi_o = 6^\circ$ where appropriate

	Spherical	Spheroidal	Molodensky spheroidal
$\| \mathbf{f} \|_4^*$	3.77×10^{-4}	3.53×10^{-4}	3.87×10^{-5}

6 Conclusions

From the theoretical developments and numerical investigations shown in the present paper, it is clear that the question as to whether terrestrial gravity data can correct a global geopotential model has been answered with a "no". This applies to the spherical, spheroidal and Molodensky-modified spheroidal kernels to a varying degree. Of note, the spherical kernels allows low-frequency terrestrial gravity data errors to pass, almost undiminished, into the geoid. The spheroidal and spheroidal Molodensky kernels attenuate these errors to a greater extent, with the spheroidal kernel being the most effective attenuator. The Molodensky-modified spheroidal kernel is slightly less effective than the spheroidal kernel because this is the price that must be paid for minimising the truncation error. However, this must be balanced against the artefact introduced by the Gibbs phenomenon that affects the spheroidal kernel.

It should be pointed out that these results only hold for the case when terrestrial gravity data are used in a spherical cap about the computation point, as is indeed customary in modern regional geoid computation. If the integration is performed over the whole Earth with any Stokes-type kernel and error-free terrestrial gravity data, then the geopotential model is always completely corrected. This holds because each approximation reduces to the original Stokes integral.

An important result is that the spheroidal and modified Stokes kernels offer a preferable approach to the spherical Stokes kernel in the presence of low-frequency terrestrial gravity data errors. These are strongly suspected to exist because terrestrial gravity data suffer from the existence of vertical datum inconsistencies between countries, systematic errors in geodetic levelling networks used to reduce the gravity observations, and irregular data coverage with some large areas devoid of data. On the other hand, the low-frequency potential coefficients that define the geopotential model are determined from the perturbations of artificial Earth satellite orbits, which are the best available source of this information. Therefore, because these low-frequency errors are not completely removed during the computation of residual gravity anomalies, it is sensible to use a low degree of modified spheroidal kernel in order to attenuate the detrimental effects of these low-frequency errors in terrestrial gravity data.

Acknowledgements. The first author is funded by an NSERC operating grant, and the second author is funded by Australian Research Council grant AA49331318 and a sabbatical leave allowance from Curtin University of Technology; all are gratefully acknowledged. The authors would also like to thank Zdeněk Martinec for providing an elegant program for computing the truncation coefficients. Finally, thanks are extended to the reviewers (Erik de Min and Lars Sjöberg) and the editor (Martin Vermeer) for their time taken to consider this manuscript.

References

Featherstone WE, Evans JD, Olliver JG (1998) A Meissl-modified Vaníček and Kleusberg kernel to reduce the truncation error in geoid computations. J Geod 72(3): 154–160

Heck B (1990) An evaluation of some of the systematic error sources affecting terrestrial gravity anomalies. Bull Geod 64: 88–108

Heck B, Grüninger W (1987) Modification of Stokes's formula by combining two classical approaches. Proc XIX IUGG general assembly, Vancouver, pp 299–337

Heiskanen WH, Moritz H (1967) Physical geodesy. Freeman, San Francisco

Meissl P (1971) Preparations for the numerical evaluation of second-order Molodensky-type formulas. Report 163, Dept of Geodetic Science and Surveying, The Ohio State University, Columbus, Ohio

Molodensky MS, Eremeev VF, Yurkina MI (1962) Methods for study of the external gravitational field and figure of the earth. Israeli Programme for the Translation of Scientific Publications, Jerusalem

Paul MK (1973) A method of evaluating the truncation error coefficients for geoidal height. Bull Geod 47: 413–425

Sideris MG, Schwarz K-P (1987) Improvement of medium and short wavelength features of geopotential solutions by local gravity data. Boll Geod Sci Aff XLVI(3): 207–221

Sjöberg LE (1984) Least squares modification of Stokes's and Vening Meinesz's formulas by accounting for the truncation and potential coefficient errors. Manuscr Geod 9: 209–229

Sjöberg LE (1986) Comparison of some methods of modifying Stokes's formula. Boll Geod Sci Aff XLV(3): 229–248

Sjöberg LE (1991) Refined least squares modification of Stokes's formula. Manuscr Geod 16: 367–375

Vaníček P, Kleusberg A (1987) The Canadian geoid – Stokesian approach. Manuscr Geod 12: 86-98

Vaníček P, Sjöberg LE (1991) Reformulation of Stokes's theory for higher than second-degree reference field and modification of integration kernels. J Geophys Res 96(B4): 6529–6539

Wong L, Gore R (1969) Accuracy of geoid heights from modified Stokes kernels. Geophys J R Astr Soc 18(1): 81–91